ARTICLE

OBC
www.rsc.org/obc

Nitric oxide release from the unimolecular decomposition of the superoxide radical anion adduct of cyclic nitrones in aqueous medium

Edward J. Locigno, Jay L. Zweier* and Frederick A. Villamena*

Center for Biomedical EPR Spectroscopy and Imaging, The Davis Heart and Lung Research Institute, and the Division of Cardiovascular Medicine, Department of Internal Medicine, College of Medicine, The Ohio State University, Columbus, OH, 43210, USA. E-mail: zweier-1@medctr.osu.edu, villamena-1@medctr.osu.edu; Fax: +1 614-247-7845; Fax: +1 614-292-8454; Tel: +1 614-247-7857; Tel: +1 614-292-8215

Received 31st May 2005, Accepted 19th July 2005
First published as an Advance Article on the web 2nd August 2005

Nitrones such as 5,5-dimethyl-1-pyrroline *N*-oxide (DMPO), 5-diethoxyphosphoryl-5-methyl-1-pyrroline *N*-oxide (DEPMPO) and 5-ethoxycarbonyl-5-methyl-1-pyrroline *N*-oxide (EMPO) have become the spin-traps of choice for the detection of transient radical species in chemical and biological systems using electron paramagnetic resonance (EPR) spectroscopy. The mechanism of decomposition of the superoxide radical anion ($O_2^{\bullet -}$) adducts of DMPO, DEPMPO and EMPO in aqueous solutions was investigated. Our findings suggest that nitric oxide (NO) was formed during the decomposition of the $O_2^{\bullet -}$ adduct as detected by EPR spin trapping using Fe(II) *N*-methyl-D-glucamine dithiocarbamate (MGD). Nitric oxide release was observed from the $O_2^{\bullet -}$ adduct formed from hypoxanthine–xanthine oxidase, PMA-activated human neutrophils, and DMSO solution of KO_2. Nitric oxide formation was not observed from the independently generated hydroxyl radical adduct. Formation of nitric oxide was also indirectly detected as nitrite (NO_2^-) utilizing the Griess assay. Nitrite concentration increases with increasing $O_2^{\bullet -}$ concentration at constant DMPO concentration, while NO_2^- formation is suppressed at anaerobic conditions. Moreover, large excess of DMPO also inhibits NO_2^- formation which can be attributed to the oxidation of DMPO to hydroxamic acid nitroxide (DMPO–X) by nitrogen dioxide (NO_2), a precursor to NO_2^-. Product analysis was also conducted to further elucidate the mechanism of adduct decay using gas chromatography-mass spectrometry (GC-MS) technique.

Introduction

Nitrones such as 5,5-dimethyl-1-pyrroline *N*-oxide (DMPO), 5-diethoxyphosphoryl-5-methyl-1-pyrroline *N*-oxide (DEPMPO) and 5-ethoxycarbonyl-5-methyl-1-pyrroline *N*-oxide (EMPO) have become an indispensable tool for the detection of transient radical species in chemical and biological systems using electron paramagnetic resonance (EPR) spectroscopy.[1–5]

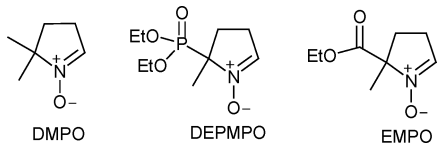

The unique characteristic of the nitrone functionality upon addition to various radicals to yield persistent radical adducts with fingerprintable EPR spectra has made nitrones a popular spin trapping reagent (Scheme 1). Superoxide radical anion ($O_2^{\bullet -}$) is among the most studied radical species due to its ability to form reactive oxygen species (ROS) such as H_2O_2 and $^{\bullet}OH$, which in unregulated concentrations, can lead to cell injury and death. The direct identification and quantification of radical species is, therefore, of critical importance in order to understand the mechanism of their formation in *in vitro* and *in vivo* systems. EPR spin-trapping using nitrones has found application in the study of kinetics and mechanisms of certain organic reactions,[6] sonolysis,[7] lipid peroxidation,[8] smoke toxicity,[9] Fenton-type reactions,[10] and *in vivo* and *in vitro* enzymatic reactions.[1,11,12] Although the use of DMPO has tremendously contributed in unravelling some of the fundamental biological processes involving radical production, it is still confronted by certain limitations such as poor $O_2^{\bullet -}$ trapping ability and the relative short half-life of the $O_2^{\bullet -}$ adduct formed, thus, making the $O_2^{\bullet -}$ adduct formation almost impossible to detect.

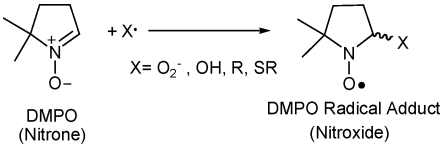

Scheme 1 Spin-trapping by DMPO.

Theoretical and experimental studies have shown that the presence of an electron-withdrawing substituent (such as the phosphoryl and alkoxycarbonyl moieties) in the C-5 position of the pyrroline ring increases the reactivity of nitrones to various radical species compared to the unsubstituted nitrone, DMPO. Moreover, the presence of intramolecular H-bonding between $O_2^{\bullet -}$ or $^{\bullet}OH$ adducts and electronic effects of the nitronyl-N in the presence of phosphoryl and alkoxycarbonyl substituents have a profound effect on the stability of the spin adduct.[5,11,13,14]

Studies on the mechanism of spin adduct decay have been previously reported on the $^{\bullet}OH$ adduct of *N*-*tert*-butyl-α-phenylnitrone (PBN), PBN–OH,[15] DMPO–OH,[16] and the hydrolysis of PBN–OH as catalyzed by Fe(III).[17] Finkelstein *et al.*[18] reported the formation of $^{\bullet}OH$ from the DMPO–OOH.

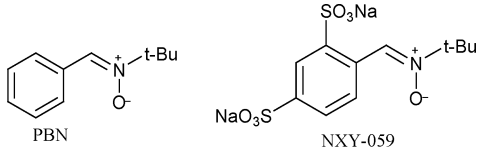

Furthermore, nitrite (NO_2^-) was reported[19] to be a product from the photodecomposition of DMPO in the presence of $^1O_2$. Other nitroso-analogues such as *N*-nitrosamines in acidic medium also liberate nitric oxide detected as NO_2^- and NO_3^-.[16,17,20] In *in vivo* systems, PBN and DMPO exhibit therapeutic properties in stroke models,[21] improvement in cerebral

DOI: 10.1039/b507530k

blood flow,[22] and NO-releasing properties.[16] The spin trap, disodium-[(*tert*-butylimino)-methyl]benzene-1,3-disulfonate *N*-oxide (NXY-059), is the first neuroprotective agent that reached clinical trial phase in the USA.[23] It is believed that the free radical trapping properties of NXY-059 is the basis of its neuroprotective action, however, experimental evidence suggests the possibility of other mechanisms being involved. The second-generation azulenyl nitrone, stilbazunenlyl nitrone (STAZN), also has exhibited neuroprotection with orders-of-magnitude higher potency than NXY-059.[24]

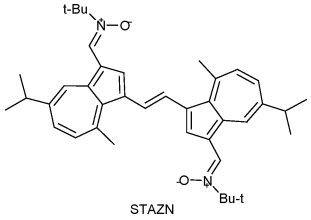

STAZN

To date, there has been no comprehensive study describing the fate of $O_2^{\bullet-}$ adducts of cyclic nitrones, specifically that of DMPO, DEPMPO and EMPO. This paper will address the mechanism of decomposition of the $O_2^{\bullet-}$ adduct of various cyclic nitrones.

Results and discussion

EPR spin trapping

The $O_2^{\bullet-}$ radical adduct (DMPO–OOH) was generated from a 1 : 2 molar ratio of DMPO and KO_2 in 40 : 60 PBS–DMSO. The resulting basic solution was adjusted either to a near neutral or acidic pH. (*Note*: The pH of 60% DMSO in PBS alone is ~10.) The solution was then purged with Ar gas, and then passed through a solution of iron (II) *N*-methyl-D-glucamine dithiocarbamate ($Fe(MGD)_2$) over a period of 60 min. Fig. 1b and 1c show the formation of NO–$Fe(MGD)_2$ complex as detected by EPR spectroscopy.[25,26] The formation of NO–$Fe(MGD)_2$ was characterized by a triplet signal with a $g_{iso} = 2.03$ G and $a_N = 12.7$ G, consistent to that reported previously for NO–$Fe(MGD)_2$ of $g_{iso} = 2.04$ G and $a_N = 12.8$ G.[27]

The increase in pH to ~12 during the formation of DMPO–OOH from DMPO and KO_2 is consistent with our theoretical prediction[28] of proton abstraction by DMPO–O_2^- in aqueous solution because of the predicted pK_a of ~15 for DMPO–OOH. No evidence of NO–$Fe(MGD)_2$ formation was observed when the pH of DMPO–OOH solution was not adjusted to either neutral or acidic pH, indicating that NO production is slow in basic medium. Nitric oxide formation became evident after the solution was adjusted to near neutral pH and the formation was slightly enhanced under acidic conditions (Fig. 1b and 1c). This may imply that nitric oxide release from the DMPO–OOH can be catalyzed in acidic medium. This increase in NO production in acidic solution may be counter intuitive considering that the half-lives for DMPO–OOH and DEPMPO–OOH are longer in acidic pH, *i.e.*, ~1.5 min and ~30 min at pH 5.6 *versus* ~1 min and ~13 min at pH 7, respectively.[3] The longer half life for $O_2^{\bullet-}$ adduct in acidic pH was also observed for 5-*tert*-butoxycarbonyl-5-methyl-1-pyrroline *N*-oxide (BocMPO), an ester analogue of EMPO (*i.e.*, ~15 min at pH 5.6 *versus* ~8.5 min at pH 7).[5] It should be noted, however, that most of the $O_2^{\bullet-}$ adduct may have already decomposed within the 30 min time period prior to the formation of NO–$Fe(MGD)_2$, and that the NO production may have been catalyzed from a decomposition product originating from the $O_2^{\bullet-}$ adduct. Nitric oxide formation was also observed within 30 min of purging solutions of either DEPMPO or EMPO in the presence of KO_2 but showed no evidence of NO formation in basic pH.

It has been previously proposed that DMPO–OOH produces $^{\bullet}$OH radical and a nonradical species, nitrosoaldehyde **2** (Scheme 2).[18] The $^{\bullet}$OH production from DMPO–OOH further supports the EPR evidence of DMPO–OOH transformation

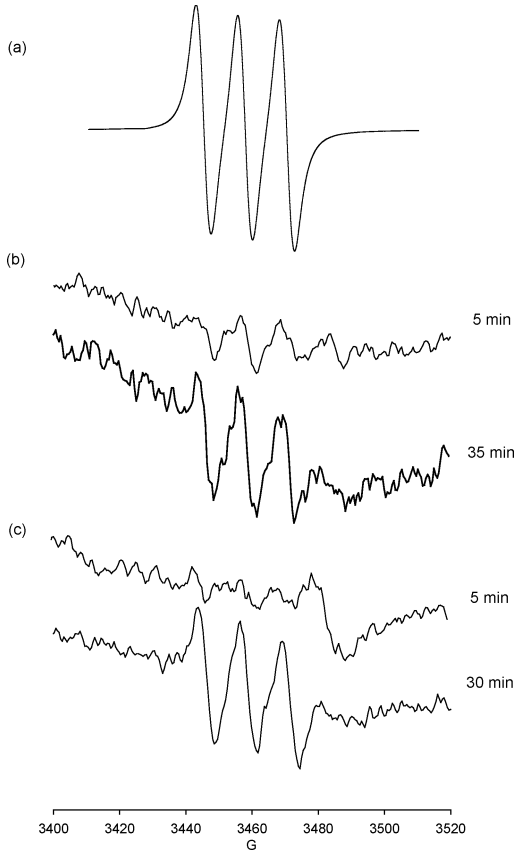

Fig. 1 X-Band EPR spectra of NO–$Fe(MGD)_2$ complex. (a) Using 10 mM $Fe(MGD)_2$ and *S*-nitroso-*N*-acetylpenicillamine (SNAP). (b) Purging argon through a solution of 28 mM DMPO and 49 mM KO_2 in PBS–DMSO at pH 6.7 as trapped by 10 mM $Fe(MGD)_2$. (c) Purging argon through a solution of 27 mM DMPO and 44 mM KO_2 in PBS–DMSO at pH 4.6 as trapped by 11 mM $Fe(MGD)_2$. See Experimental section for spectrometer settings. All spectra are scaled the same except for (a).

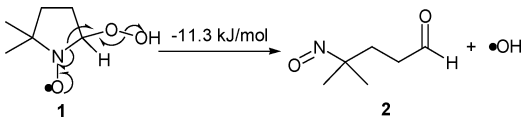

Scheme 2 Unimolecular decomposition of DMPO–OOH.

to DMPO–OH. Our results[29] using density functional theory (DFT) at the B3LYP/6-31+G**//B3LYP/6-31G* level indicate an exoergic free energy of reaction for Scheme 2 of $\Delta G_{rxn,298K} = -11.3$ kJ mol^{-1} for DMPO–OOH and -8.0 kJ mol^{-1} for DEPMPO–OOH. These values are even more favorable in aqueous system at the PCM/B3LYP/6-31+G**//B3LYP/6-31G* level with $\Delta G_{rxn,298K}$ of -26 kJ mol^{-1} for DMPO–OOH and -25.5 kJ mol^{-1} for DEPMPO–OOH. Therefore, acid catalyzed decomposition of **2** to yield NO may occur *via* protonation of the nitroso-O, followed by elimination reaction to form the keto-aldehyde, and subsequent homolytic cleavage of NO–H bond to give nitric oxide and H-atom as shown in Scheme 3. The calculated bond dissociation enthalpy at the B3LYP/6-31+G**//B3LYP/6-31G* level for NO–H was found to be about 35.6 kJ mol^{-1} indicating that NOH is likely to dissociate to NO and H radicals. Evidence of protonation of nitroso-O has been observed in solution for 1-benzyl-4-nitroso-5-aminopyrazole.[30] The formation of DMPO–H adduct arising

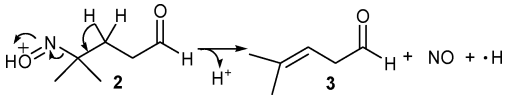

Scheme 3 Acid-catalyzed formation of NO.

from the addition of $^{\bullet}H$ to DMPO was not experimentally observed due, perhaps, to a more thermodynamically preferred reaction of $^{\bullet}H$ in solution, *e.g.*, H-atom abstraction and addition as well as radical–radical coupling reactions with $^{\bullet}OH$, $O_2^{\bullet-}$, or $^{\bullet}H$, *etc.*

Aliphatic *C*-nitroso compounds such as 2-methyl-2-nitrosopropane (MNP) and its electron-withdrawing substituted derivatives have exhibited NO donating capability due to their instability (C–N bond dissociation energy is 150–167 kJ mol^{-1}), similar to those of O–NO and O–NO_2 bonds in nitrite and nitrate esters.[31] Calculated C–N bond length for nitroso-aldehyde **2** is relatively long, *i.e.*, 1.52 Å,[13,32] suggesting that the homolytic C–N bond scission can lead to the formation of NO and $R^{\bullet}$.

To confirm if NO production originates exclusively from the $O_2^{\bullet-}$ radical adduct, other known $O_2^{\bullet-}$ generating systems such as PMA-activated neutrophils and hypoxanthine–xanthine oxidase (HX–XO)[33] were employed. The formation of NO–$Fe(MGD)_2$ was observed using PMA-activated neutrophils and DMPO at neutral pH (Fig. 2a), and from the solution of 0.6 μM XO in PBS–DTPA, 40 mM DMPO and 80 mM HX at pH 6.1 (Fig. 2b). The rate of $O_2^{\bullet-}$ flux from the HX–XO system employed was calculated to be 28.3 ± 2.4 μM min^{-1}. The formation of the NO–$Fe(MGD)_2$ complex was also observed using DEPMPO as a spin trap in the presence of HX–XO, or PMA-activated neutrophils $O_2^{\bullet-}$ generating systems. The nature of the fourth peak that appears at the highest field in some of the spectra is unknown at the moment since the oxidized $Fe(MGD)_2$ alone did not show any signal in this region and its intensity remained unchanged overtime. This phenomenon has been observed previously[26] but no explanation on its nature was ever discussed in detail.

Alternatively, $Fe(MGD)_2$ was directly added to a solution of 25 mM DMPO and 50 mM KO_2 in PBS–DMSO at pH 8.1 (Fig. 2c) and immediate formation of an EPR signal due to NO–$Fe(MGD)_2$ was observed. This instantaneous formation of EPR signal indicates that Fe^{2+} may catalyze the NO formation. The formation of NO–$Fe(MGD)_2$ was also observed when $Fe(MGD)_2$ was directly added to a solution of DEPMPO or EMPO in the presence of KO_2.

The production of NO from DMPO–OH was also investigated, since experimental evidence showed that the $^{\bullet}OH$ adduct is formed from the decomposition of the $O_2^{\bullet-}$ adduct.[34] DMPO–OH was generated from a solution of DMPO, $FeSO_4$ and H_2O_2 at pH 7.0. The solution of DMPO–OH was purged with Ar and bubbled through a solution of $Fe(MGD)_2$ and showed no indication of formation of NO–$Fe(MGD)_2$ over the 30 min time period. The formation of NO–$Fe(MGD)_2$ complex was not observed as well from the generated $^{\bullet}OH$ adducts of DEPMPO or EMPO at pH 6.6 indicating that NO formation exclusively originates from $O_2^{\bullet-}$ adduct.

Attempts to directly detect NO formation using electrochemical and chemiluminescence techniques gave inconclusive results due to the slow release of NO in solution and high signal interference from DMSO. The formation of peroxynitrite[35] from the reaction of NO and $O_2^{\bullet-}$ was also investigated in which the $O_2^{\bullet-}$ adduct was incubated in the presence of tyrosine. Using high-performance liquid chromatographic technique,[36] and authentic samples of nitrotyrosine, the concentration of nitrotyrosine formed was found to be below the detection limit of the electrochemical and UV detectors used. This indicates that NO reaction with $O_2^{\bullet-}$ to form peroxynitrite may not be the major pathway for NO decomposition in solution due to the slow release of NO relative to the rate of $O_2^{\bullet-}$ dismutation in solution.

Control experiments were performed to confirm if there are any other possible sources for NO. Individual solutions of 23 mM KO_2, 5.7 mM H_2SO_4 or 28 mM DMPO in 40% DMSO–PBS (pH 6.7), 28 mM DMPO in PBS (pH 6.6), or DMSO alone showed no evidence of NO formation after 30 min of purging. Solution of 100 mM $NaNO_2$ in 10% DMSO–PBS (pH 7.3), gave no evidence of NO formation using the same procedure as above, while acidification of this solution to pH 6.8 showed formation of NO with S/N = 4 within only 5 min of purging.

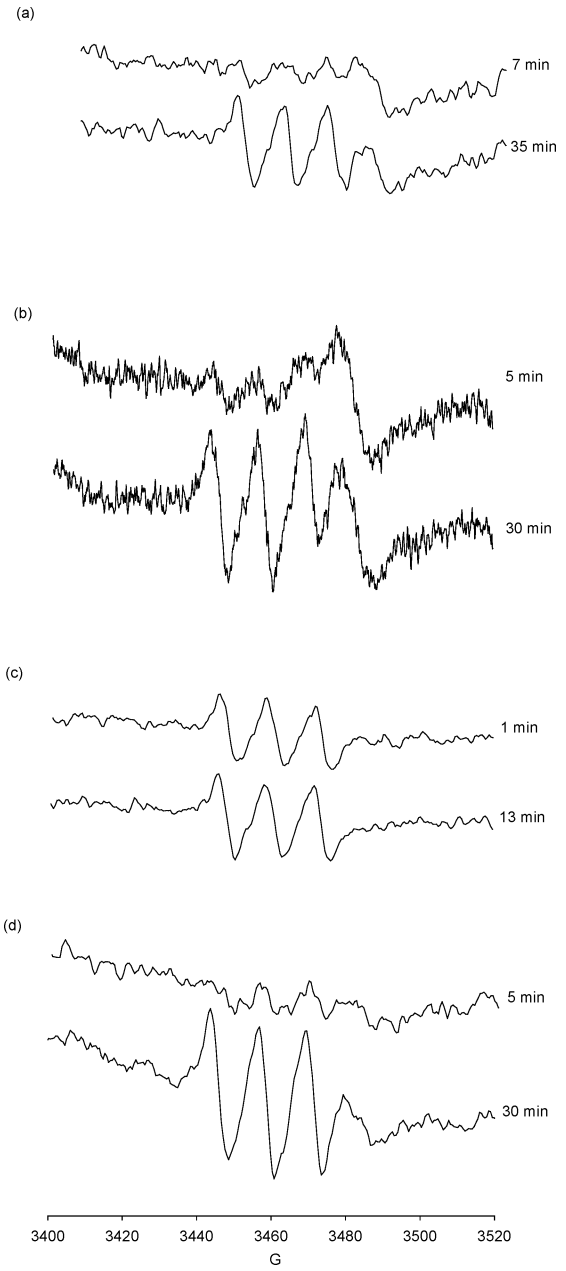

Fig. 2 X-Band EPR spectra of NO–$Fe(MGD)_2$ complex. (a) Purging argon through an incubated solution composed of 49 mM DMPO using PMA-activated human neutrophils at pH 6.7 as trapped by 11 mM $Fe(MGD)_2$. (b) Purging argon through an incubated solution of 2.5 mL PBS solution of 40 mM DMPO, 0.6 μM XO and 80 mM HX solution, as trapped 10 mM $Fe(MGD)_2$. (c) Direct addition of 3 mM $Fe(MGD)_2$ to a solution of 17 mM DMPO and 33 mM KO_2 in PBS–DMSO at pH 8.1. (d) Purging argon through a solution of 27 mM DEPMPO and 49 mM KO_2 in PBS–DMSO at pH 7.0 as trapped by 10 mM $Fe(MGD)_2$. See Experimental section for spectrometer settings. All spectra were scaled the same. The sweep widths are 500 G for (a), (c) and (d); and 120 G for (b).

No indication of NO formation was observed by directly mixing a solution of $Fe(MGD)_2$ to individual solutions of 17 mM DMPO (pH 5.5 or 9.4) or 31 mM KO_2 (pH 6.9 or 12.8). Also, using the same direct mixing method, no NO release was observed from combinations of spin trap with individual components of the various $O_2^{\bullet-}$ generating systems such as HX–XO or PMA-neutrophils after incubation for 15 minutes (*Note:* no pH adjustments were done). However, NO formation

was observed from directly mixing $Fe(MGD)_2$ to solutions of nitrones in the presence of all the components of various $O_2^{\bullet-}$ generating system.

Nitrite assay

The reaction of NO with O_2 can lead to the formation of reactive nitrogen species (RNS) such as NO_2, N_2O_4, and N_2O_3 which can hydrolyze in water to form NO_2^-.[37] Since the formation of peroxynitrite was not previously observed, we instead hypothesized that NO may react with molecular O_2 to undergo a one-electron oxidation to form nitrite (NO_2^-). Nitrite formation was investigated by Griess assay.[38] Fig. 3 (inset) shows the dependence of NO_2^- formation as a function of HX concentration after 12 h of incubation in the presence of XO and/or DMPO. In this experiment, the rate of $O_2^{\bullet-}$ flux from 0.13 μM XO was calculated to be 8.2 ± 2.5 μM min^{-1}. As shown in Fig. 3, only background absorption was observed from individual or a combination of two components from the HX–XO $O_2^{\bullet-}$ generating system. Fig. 4 shows that NO_2^- can also be formed from DMPO–KO_2 system and that NO_2^- can be attenuated with increasing KO_2 concentration at constant DMPO concentration.

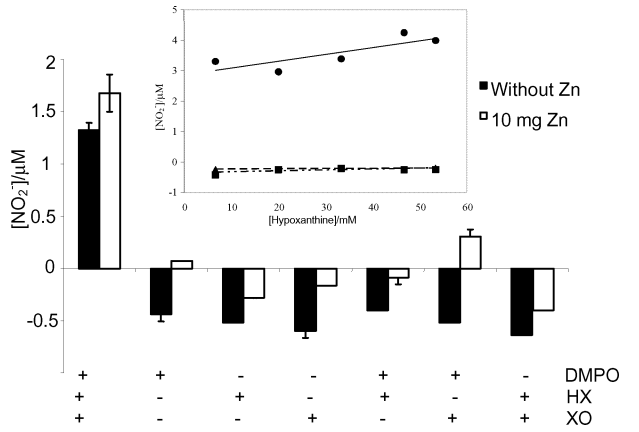

Fig. 3 Griess assay of nitrite formation using 100 mM DMPO, 0.13 μM xanthine oxidase (XO) and 22 mM hypoxanthine (HX); (Inset) Nitrite formation as a function of HX concentration using (●) 100 mM DMPO and 0.13 μM XO; (■) 0.13 μM XO alone; and (▲) 100 mM DMPO alone after 12 h incubation at room temperature. Measurements were done in triplicate.

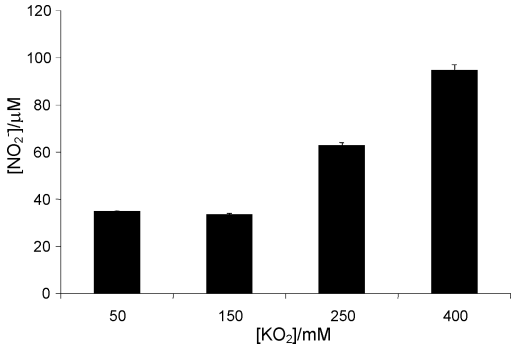

Fig. 4 Griess assay of nitrite formation from various concentrations of KO_2 using 100 mM DMPO in PBS–DMSO solution after 12 h incubation at ambient temperature. Measurements were done in triplicate.

Conversely, Fig. 5 shows that the formation of NO_2^- can be inhibited in the presence of excess DMPO at constant KO_2 concentration. This indicates that an intermediate leading to the formation of NO_2^- is quenched by excess DMPO. A possible intermediate for NO_2^- is nitrogen dioxide (NO_2) which can be formed from the reaction of NO with O_2. Nitrogen dioxide is a known oxidizing agent and has been found to oxidize DMPO,

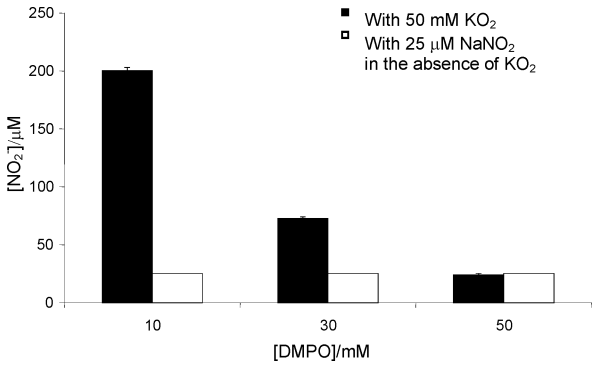

Fig. 5 Griess assay of nitrite formation from various concentrations of DMPO with 50 mM KO_2 in PBS–DMSO solution after 12 h incubation at ambient temperature. Measurements were done in triplicate.

into an acyl nitroxide (DMPO–X).[39] Chlorine dioxide radical (ClO_2) which is isoelectronic to NO_2 can also oxidize DMPO to give DMPO–X and hypochlorous acid (HClO).[40] To further verify if NO_2 can indeed oxidize DMPO, a solution of 732 mM DMPO in PBS–DTPA was purged for 1 min with 1% NO_2 in N_2. The solution gave a seven-line EPR spectrum with hyperfine splitting constants of $a_N = 7.27$ G, $a_H = 4.1$ G, consistent with that reported for DMPO–X.[4] The NO_2-bubbled DMPO solution was then extracted with chloroform and GC-MS analysis of the extract revealed a nominal peak at 129 m/z (corresponding to the [DMPO–X + H^+]) and a retention time of 4.85 min. GC-MS analysis of the chloroform extract from the incubated solution of 25 mM DMPO, 50 mM KO_2 and 50 mM hydrochloric acid gave a new peak at 4.80–4.85 min with a similar mass fragmentation pattern observed for [DMPO–X + H^+] generated from NO_2 and DMPO solution. Therefore, it can be proposed that DMPO–X is produced from the direct oxidation of DMPO by NO_2 with perhaps HNO as a by-product-analogous to the pathway of ClO_2 oxidation of DMPO as previously reported.[40] The formation of nitroxyl, HNO, was not detected however, due to its ability to spontaneously self-dismutate[41] to form N_2O and water [eqn (1)]. It is also possible for O_2 to be reduced by HNO to form hydrogen peroxide and nitric oxide[39,41] [eqn (2)], but this was not pursued in this study.

$$2HNO \rightarrow HON{=}NOH \rightarrow N_2O + H_2O \quad (1)$$

$$HNO \xrightarrow{O_2} NO + H_2O_2 \quad (2)$$

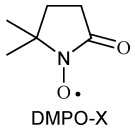

DMPO-X

To examine the effect of DMPO concentration on Griess analysis of NO_2^-, 10, 30 and 50 mM DMPO was incubated with 25 μM $NaNO_2$ for 12 h at ambient temperature. Results show that nitrite concentration was not affected by DMPO concentration indicating that DMPO does not affect NO_2^- concentration during analysis (Fig. 5). Product analysis of the mixture with 1 : 1 and 1 : 2 molar ratio of DMPO–KO_2 after 12 h of incubation, gave the same GC-MS profile.

The maximum EPR signal intensity of the $O_2^{\bullet-}$ adduct formed from DMPO–KO_2 in PBS–DMSO was double integrated and quantified using 1 μM TEMPO as standard. The calculated superoxide adduct concentration from 50 mM–50 mM (DMPO : KO_2) was ~29 μM, while ~12 μM was calculated from both 50 mM–25 mM or 25 mM–50 mM concentrations. It can be assumed that the amount of NO generated is directly dependent on the concentration of the adduct formed, while the amount of adduct formed is inversely proportional to the

amount of NO_2^- generated, indicating that DMPO is highly reactive towards NO_2.

The effect of acid on the nitrite formation during incubation of DMPO–OOH solution was also investigated. Prior to NO_2^- analysis, solutions were purged with Ar to remove excess NO that may have been produced during the non-enzymatic reduction of NO_2^-.[42] Results show that by increasing the HCl concentration (0–80 mM), a decrease in NO_2^- concentration can be observed using 100 mM DMPO and 50 mM KO_2 (Fig. 6). The same behavior was also observed from the generated $O_2^{\bullet-}$ adduct of DEPMPO under the same experimental conditions. This observation is consistent with previous study[43] showing that NO_2^- decomposes to NO and NO_2 under acidic conditions.

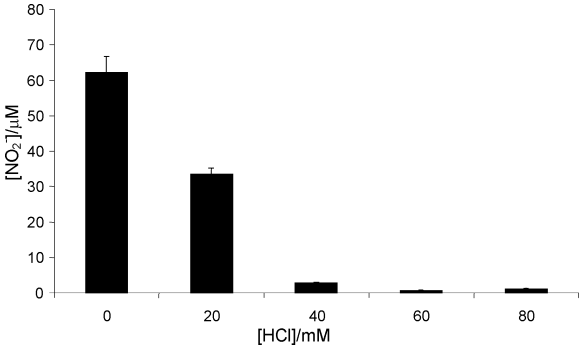

Fig. 6 Griess assay of nitrite formation from 100 mM DMPO and 50 mM KO_2 in PBS–DMSO after 12 h incubation in the presence of various concentrations of HCl at ambient temperature. Measurements were done in triplicate.

To examine if nitrate (NO_3^-) is also formed along with NO_2^- from the incubated solution of DMPO–OOH, Zn metal[44] was added prior to NO_2^- analysis. Fig. 7 shows that there is no significant increase in NO_2^- concentration after the addition of Zn to an incubated solution of DMPO and KO_2 in PBS–DMSO. The same result was also observed using the HX–XO $O_2^{\bullet-}$ generating system. Moreover, reaction of Zn with DMPO, KO_2, XO, or HX alone did not show any increase in the background NO_2^- concentration. This insignificant increase in NO_2^- concentration in the presence of Zn metal indicates that NO_2^- and not NO_3^-, is the predominant decomposition product of NO. This observation further supports our previous finding that peroxynitrite is not the major product of NO decomposition.

$$\text{DMPO} + {}^{\bullet}\text{OH} \rightarrow \text{DMPO–OH} \quad (3)$$

$${}^{\bullet}\text{OH} + \text{DMSO} \rightarrow {}^{\bullet}\text{CH}_3 + \text{CH}_3\text{S(O)OH} \quad (4)$$

$$\text{DMPO} + {}^{\bullet}\text{CH}_3 \rightarrow \underset{\mathbf{4}}{\text{DMPO-CH}_3} \quad (5)$$

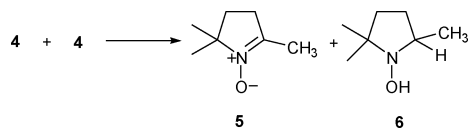

5 **6** (6)

$$\text{DMPO} + {}^{\bullet}\text{OCH}_3 \rightarrow \underset{\mathbf{7}}{\text{DMPO-OCH}_3} \quad (7)$$

$$\text{DMPO–O} + {}^{\bullet}\text{CH}_3 \rightarrow \mathbf{7} \quad (8)$$

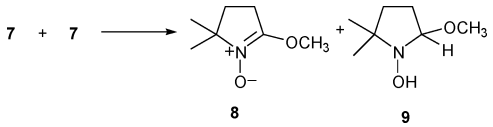

8 **9** (9)

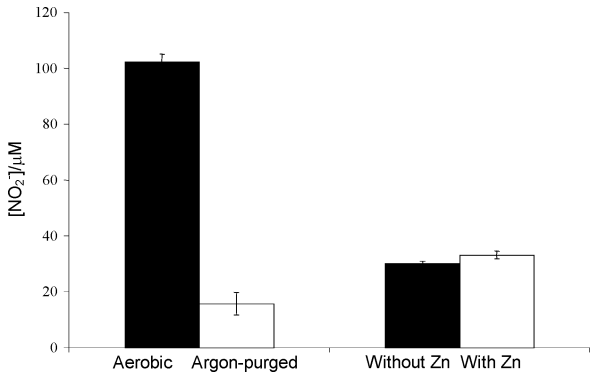

Fig. 7 Effect of O_2 and Zn on nitrite formation from solutions of 100 mM DMPO with 50 mM KO_2 in PBS–DMSO solution after 12 h incubation at ambient temperature using Griess assay. Measurements were done in triplicate.

The effect of O_2 on the formation of NO_2^- was also investigated to confirm if NO_2^- originates from the reaction of NO and O_2 *via* formation of nitrogen oxides and their subsequent hydrolysis.[37] Results show that incubation of DMPO–OOH exposed to air gave significantly higher NO_2^- concentration compared to a solution which was anaerobically incubated (Fig. 7). This O_2-dependent NO_2^- formation further demonstrates that NO_2^- is derived from NO.

The effect of superoxide dismutase (SOD) was investigated to confirm if $O_2^{\bullet-}$ is essential to the formation of NO. Results show that by using HX–XO $O_2^{\bullet-}$ generating system (8.2 ± 2.5 μM $O_2^{\bullet-}$ min^{-1}) and 50 mM DMPO, the formation of NO_2^- was inhibited in the presence of SOD (33 units mL^{-1}) while significant amount of NO_2^- (0.92 μM) was formed in the absence of SOD (see Experimental section). No NO_2^- formation was observed from SOD solution alone as well as from solutions containing a combination of SOD–DMPO, SOD–XO or SOD–HX, or SOD with DMPO–XO, DMPO–HX or XO–HX. The inhibition of NO_2^- formation in the presence of SOD further demonstrates that the presence of $O_2^{\bullet-}$ is essential to the formation of NO_2^-.

Nitrite formation from the generated DMPO–OH adduct was also investigated. No observable amount of NO_2^- was formed from solutions of 25 mM DMPO in the presence of 11 mM H_2O_2 and 22 mM $FeSO_4$, or using these similar components in the presence of an acid. The formation of NO_2^- was also investigated from DMPO–H_2O_2, DMPO–$FeSO_4$, or $FeSO_4$–H_2O_2 but these combinations yielded no NO_2^-, consistent with the spin trapping experiments mentioned above.

Product analysis

Gas chromatography-mass spectrometric technique (GC-MS) was employed to analyze the decomposition products of DMPO–OOH. Product analysis after 12 h of incubation of 25 mM DMPO and 50 mM KO_2 in DMSO–PBS at pH 11 indicates that most of the DMPO remained unreacted and the molecular ion mass corresponding to **2** was not detected. However, 2 distinctive GC peaks were evident corresponding to α-substituted-methyl DMPO **5** and α-substituted-methoxy DMPO **8** with molecular ion peaks of 127 *m/z* EI (128 *m/z* by CI) and 143 *m/z* EI (144 *m/z* by CI), respectively. Previous studies show that bimolecular decomposition of radical adducts of cyclic nitrones can occur to give the corresponding nitrone and hydroxylamine[29] [eqn (6) and (9)]. The hydroxylamines **6** and **9** were not detected using GC-MS due perhaps to their instability at high temperature.

The formation of compounds **5** and **8** may have originated from $^{\bullet}OH$ which can be generated either from H_2O_2 (*via* the dismutation of $O_2^{\bullet-}$), or DMPO–OOH *via* mechanism shown in Scheme 2. Theoretical calculations using DFT at the

B3LYP/6-31+G**//B3LYP/6-31G* level for the homolytic O–O bond cleavage gave an endoergic free energy of reaction of $\Delta G_{rxn,298K}$ = 154.1 kJ mol^{-1} for H_2O_2, and 115.1 (triplet) or 79.1 (singlet) kJ mol^{-1} for DMPO–OOH.[29] It can therefore be proposed that there may be 2 possible pathways for the formation of DMPO–OCH_3 adduct **7**, *i.e.*, from direct addition of $^{\bullet}OCH_3$ to DMPO [eqn (7)], or *via* radical–radical reaction of DMPO–O$^{\bullet}$ and $^{\bullet}CH_3$ [eqn (8)].

In Fig. 8a, the peak found at 5.1 min which corresponds to **5** was not observed in acidic condition (Fig. 8b). The inhibitive effect of acid on the formation of nitrone **5** is unclear at the moment, but it may be assumed that the bimolecular decomposition of adduct **4** is less favorable than that of **7** since compound **8** was formed in acidic condition.

However, two new distinct peaks were observed after DMPO–OOH was incubated in acidic conditions (Fig. 8b) with retention times of 4.7 min and 6.0 min, corresponding to $[M + H]^+$ peaks of 99 m/z and 115 m/z (EI), respectively. These $[M + H]^+$ peaks were also confirmed by CI. A common ion at 29 m/z can be observed in both EI spectra, characteristic of an aliphatic aldehyde. It is therefore proposed that the 99 m/z and 115 m/z $[M + H]^+$ correspond to products **10** and **11**, respectively. Possible mechanisms for the formation of compounds **10** and **11** may be from elimination and radical–radical addition reactions of nitroso-aldehyde **2**, respectively, as shown in Scheme 4.

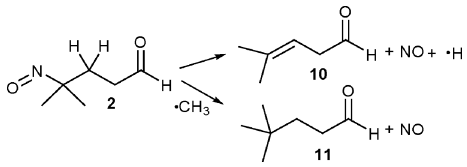

Scheme 4 Elimination and radical–radical addition reactions of nitroso-aldehyde.

Conclusion

EPR spin-trapping studies and NO_2^- analysis show that NO is a decomposition product of the $O_2^{\bullet-}$ adduct of the spin-traps, DMPO, DEPMPO and EMPO and was further supported by product analysis. Scheme 5 shows a summary of the proposed overall mechanism for the decomposition of DMPO–OOH in aqueous solution. The mechanism of NO formation proceeds *via* unimolecular decomposition of the $O_2^{\bullet-}$ adduct to form the nitroso-aldehyde and subsequent release of NO. The formation of NO was also observed using other $O_2^{\bullet-}$ generating systems such as HX–XO and PMA-activated human neutrophils in the presence of spin traps. Nitric oxide generation was not observed from independently prepared $^{\bullet}OH$ adducts. The formation of NO was observed in both acidic and neutral pH, while NO release is inhibited in basic medium. The fate of NO proceeds *via* oxidation by O_2 to form the NO_2 radical which can then

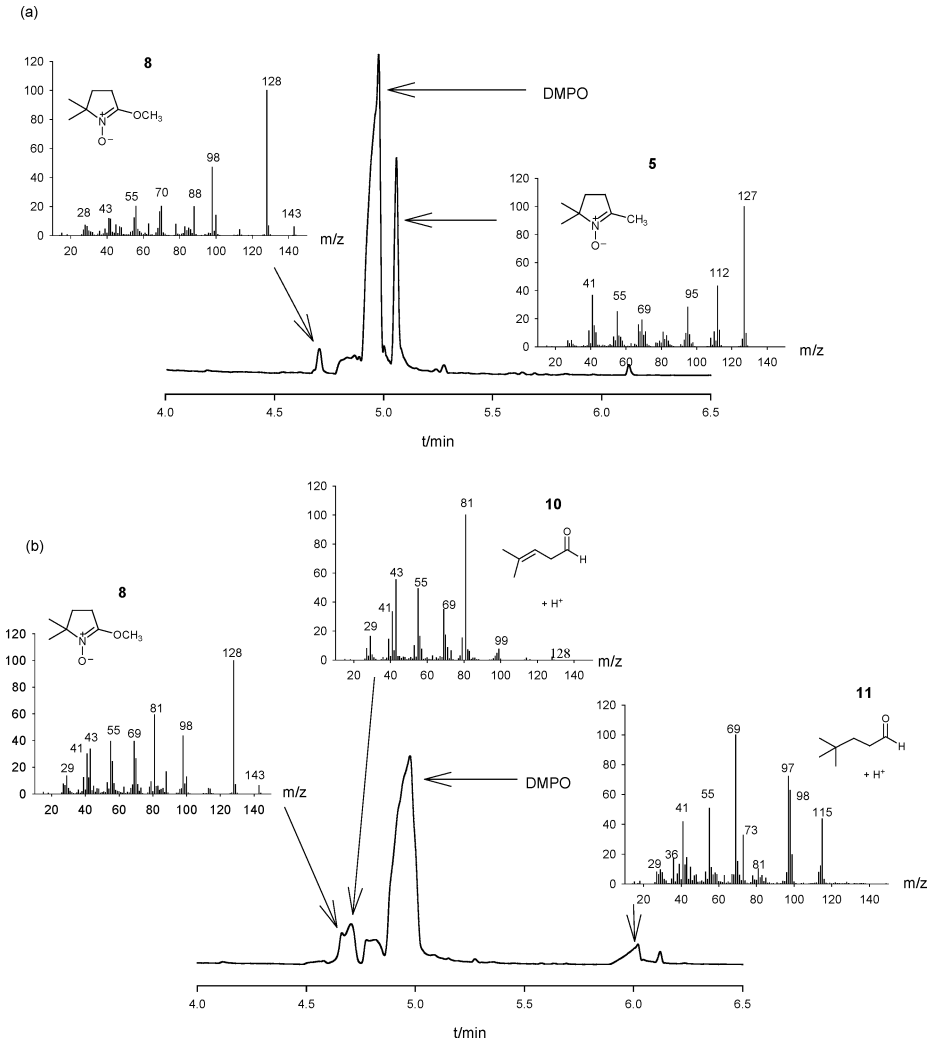

Fig. 8 GC-MS of products of the decomposition of the superoxide adduct of DMPO using electron ionization. (a) Analysis of chloroform extract of solution of 25 mM DMPO and 50 mM KO_2 in deionized water incubated over a 12 h period at ambient temperature at pH 11. (b) Analysis of chloroform extract of a solution of 25 mM DMPO, 50 mM KO_2, and 50 mM HCl in deionized water incubated over a 12 h period at ambient temperature.

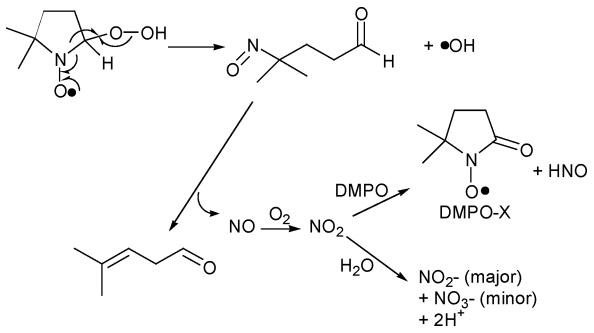

Scheme 5 Proposed overall mechanism of decay of DMPO–OOH.

either decompose to NO_2^- or react with excess DMPO to form DMPO–X and HNO. Nitrite formation was found to be dependent on the DMPO and KO_2 concentrations as well as O_2 and pH. There was no evidence of peroxynitite formation from the reaction of NO with $O_2^{\bullet -}$, indicating that $O_2^{\bullet -}$ dismutation is faster than NO release from the nitroso-aldehyde intermediate. Although NO generation may also originate indirectly from other sources such as from the bimolecular decomposition products or other modes of unimolecular decomposition, the results presented in this study are, by far, in agreement with available theoretical and experimental data.

Experimental

Materials

The nitrones DMPO, DEPMPO, and EMPO were obtained from the Alexis Biochemical Corporation (Switzerland) and were used without further purification. Sodium *N*-methyl-D-glucamine dithiocarbamate (MGD) was synthesized using the procedure developed by Shinobu, *et al.*[45] The *N*-methyl-D-glucamine and carbon disulfide utilized for MGD synthesis were purchased from Aldrich (Wisconsin, USA). $FeNH_4SO_4$, HX, and SOD were obtained from the Sigma-Aldrich Corporation (San Diego, Caifornia USA). Dulbelcco's phosphate-buffered saline (PBS) was used and contained 100 μM diethylenetriaminepentaacetic acid (DTPA) as a metal chelating agent.

Griess assay was carried out using sulfanilamide, *N*-1-naphthylethylenediamine dihydrochloride[46], and $NaNO_2$ standard (Promega Corporation, Wisconsin, USA). Xanthine oxidase (from bovine milk) with a protein concentration of 10.5 mg mL^{-1} and activity of 14.43 U mL^{-1} was obtained from Calbiochem (Germany).

Preparation of the $Fe(MGD)_2$ complex

Freshly prepared $Fe(MGD)_2$ was used in all the studies by dissolving 76 mg of MGD in 10 mL distilled water. The solution was then purged with Ar gas for ~5–10 min and 39 mg of $FeNH_4SO_4$ was added. $Fe(MGD)_2$ gave a clear yellowish solution which oxidizes to a dark brown solution.[26]

EPR Measurements

EPR measurements were carried out on a Bruker EMX Spectrometer equipped with HS resonator. General instrument settings, unless otherwise indicated, are as follows: microwave power, 20 mW; modulation amplitude, 4.00 G; receiver gain, 1.00×10^5; scan time, 42 s; time constant, 82 ms; sweep width 500 G. Measurements were performed using a 50 μL capillary tube.

Spin trapping of $O_2^{\bullet -}$

(a) KO_2 generating system.

Method I.

Purging with argon. Superoxide adduct was generated in a 5 mL conical flask by adding 1.5 mL DMSO solution of 116 mM KO_2 to a 1 mL PBS solution of 100 mM DMPO. It should be noted that the pH of PBS with 60% DMSO alone is ~10, while the pH was measured to be 12–13 in the same solvent system in the presence of DMPO and KO_2. The pH was therefore adjusted to 6.7 by adding ~1.0 mL of 100 mM H_2SO_4. The flask was covered with rubber septa and purged with Ar using a needle syringe. The purged gas was allowed to flow through a tube connected to a separate reaction vessel containing 2 mL of 10 mM $Fe(MGD)_2$. EPR spectrum was obtained for each 50 μL $Fe(MGD)_2$ aliquot taken at various time intervals. This procedure was repeated using 95 mM DEPMPO or 105 mM EMPO in PBS at pH 7.

Method II.

Direct mixing. Superoxide adduct was generated by mixing 25 μL of 100 mM DMPO in PBS and 50 μL of 100 mM KO_2 in DMSO. The pH of the solution was then adjusted to ~6.5 by adding ~25 μL of 100 mM H_2SO_4. To the resulting solution, 50 μL of 10 mM $Fe(MGD)_2$ was added and the EPR spectrum was immediately obtained. This procedure was repeated using 100 mM DEPMPO, or with 105 mM EMPO at pH 6.5. *Note*: Addition of $Fe(MGD)_2$ causes the pH to increase to 8.1 for DMPO, 7.4 for DEPMPO, and 7.8 for EMPO.

(b) Xanthine oxidase and hypoxanthine generating system. A 2.5 mL mixture containing 0.6 μM XO, 80 mM HX and 40 mM DMPO was allowed to incubate for 15 min before purging with Ar. Method I was employed for the detection of NO formation.

(c) PMA-activated neutrophils. Superoxide adduct was generated by adding 50 μL of 10 nM phorbol myristate acetate (PMA) to a 1 mL PBS solution of 49 mM DMPO and isolated human neutrophils (~10^9 mL^{-1}). The mixture was allowed to incubate for 15 min before purging with Ar. Method I was employed for the detection of NO formation.

Spin trapping of $^{\bullet}OH$

Hydroxyl radical adduct was generated from a 3.0 mL solution containing 15 mM H_2O_2, 50 mM DMPO and 65 mM $FeSO_4$. The pH was adjusted to 7.0 by adding 4.5 μL of 1 M H_2SO_4. Method I was employed for the detection of NO formation. This procedure was repeated from solutions of 50 mM DEPMPO or 105 mM EMPO in PBS at pH 6.7.

Griess assay

(a) KO_2 generating system. In a typical 96-well cell culture cluster, a 50 μL PBS–DMSO solution of 100 mM DMPO and 50 mM KO_2 was incubated for 12 h at ambient temperature prior to the analysis. 50 μL of sulfanilamide was added and the solution was allowed to incubate for 5 min away from light. After incubation, 50 μL of NED was then added and the solution was then allowed to incubate for additional 5 min. Absorbance at 550 nm was obtained using a Beckman Coulter AD Model 340. Using $NaNO_2$ standard solution, the NO_2^- concentrations were obtained. This procedure was repeated using varying concentrations of DMPO at 300, 500, and 800 mM each containing 50 mM KO_2, or by using 150, 250, and 400 mM KO_2 each with 100 mM DMPO.

(b) Xanthine oxidase and hypoxanthine generating system. Same as in (a) but using 50 μL PBS solution consisting of 0.13 μM XO, 100 mM DMPO, and 22 mM HX.

(c) Zinc reduction. Approximately 10 mg of Zn dust was added to each of the solutions used in (a). The solutions were then allowed to incubate for 3 h, centrifuged, and the supernatant removed and filtered using a 0.13 micron filter. Griess assay was performed as in (a).

(d) Effect of SOD. Same as in (a) but using 50 μL solution of 1.3 μM XO, and addition of 20 μL SOD (328 U mL^{-1}), 30 μL PBS and 50 μL of 110 mM HX. The resulting solution was allowed to incubate for 2 min and 50 μL of 200 mM DMPO

was added. The resulting 200 μL of solution was then allowed to incubate over a 12 h period.

Rate of superoxide generation and quantification of superoxide adduct

The rate of $O_2^{\bullet -}$ production was determined spectrophotometrically at 550 nm by monitoring the initial rate of reduction of 40 μM cytochrome c in the presence of 0.6 μM XO and 88 mM HX, or from 0.13 μM XO and 22 mM HX. The concentration of $O_2^{\bullet -}$ was derived from the [Fe^{2+}] using the molar extinction coefficient (19 500 M^{-1} cm^{-1}).[47]

The $O_2^{\bullet -}$ adduct formed from various concentrations of KO_2 and DMPO was quantified by double integration of the EPR spectrum and concentrations were calculated from 1 μM TEMPO standard solution.

Nitrogen dioxide reaction with DMPO

A solution of 730 mM DMPO in PBS was purged with 1% NO_2 – 99% N_2 for 1 min and the EPR spectrum was obtained.

Gas chromatography-mass spectrometry

GC-MS analysis was carried out on a Flennigan TraceGC Ultra and Trace DSQ equipped with positive ion electron impact ionization (EI) and chemical ionization (CI) modes. In a typical experiment, 1.5 mL water–DMSO solution of 25 mM DMPO, 50 mM KO_2 and 50 mM hydrochloric acid was extracted with two 1 mL portions of HPLC grade chloroform. Two μL of chloroform extract was injected into the column at an initial temperature of 40 °C using a ramp of 20 °C min^{-1} up to a maximum temperature of 250 °C. MS detection was conducted at 200 °C ion source temperature, electron energy of 70 eV, and scan speed of 1.6584 scans s^{-1} or 1.8832 scans min^{-1} for EI and CI measurements, respectively.

Acknowledgements

This work was supported by NIH Grants HL38324, HL63744, and HL65608. The authors would like to thank Dr Murugesan Velayutham for helpful discussions.

References

1 J. L. Zweier, P. Kuppusamy and G. A. Lutty, *Proc. Natl. Acad. Sci. USA*, 1988, **85**, 4046; J. L. Zweier, P. Kuppusamy, R. Williams, B. K. Rayburn, D. Smith, M. L. Weisfeldt and J. T. Flaherty, *J. Biol. Chem.*, 1989, **264**, 18890.
2 K. Stolze, N. Udilova and H. Nohl, *Biochem. Pharmacol.*, 2002, **63**, 1465; G. Olive, A. Mercier, F. Le Moigne, A. Rockenbauer and P. Tordo, *Free Radical Biol. Med.*, 2000, **28**, 403.
3 B. Tuccio, R. Lauricella, C. Frejaville, J.-C. Bouteiller and P. Tordo, *J. Chem. Soc., Perkin Trans. 2*, 1995, 295.
4 G. M. Rosen, B. E. Britigan, H. J. Halpern and S. Pou, *Free Radicals: Biology and Detection by Spin Trapping*, Oxford University Press, New York, 1999.
5 F. Villamena and J. Zweier, *J. Chem. Soc., Perkin Trans. 2*, 2002, 1340.
6 C. X. C. Santos, E. I. Anjos and A. Ohara, *Arch. Biochem. Biophys.*, 1999, **372**, 285; R. U. Rojas Wahl, L. Zeng, S. A. Madison, R. L. DePinto and B. J. Shay, *J. Chem. Soc., Perkin Trans. 2*, 1998, 2009; C. A. Jenkins, D. M. Murphy, C. C. Rowlands and T. A. Egerton, *J. Chem. Soc., Perkin Trans. 2*, 1997, 2479.
7 V. Misik and P. Reisz, *Ultrason. Sonochem.*, 1996, **3**, S173.
8 C. Lai and L. H. Piette, *Biophys. Res. Commun.*, 1977, **78**, 51–59; S. I. Dikalov and R. P. Mason, *Free Radical Biol. Med.*, 2001, **30**, 187; K. Stolze, N. Udilova and H. Nohl, *Free Radical Biol. Med.*, 2000, **29**, 1005.
9 L.-Y. Zhang, K. Stone and W. A. Pryor, *Free Radical Biol. Med.*, 1995, **19**, 161.
10 L. Gianni, J. Zweier, A. Levy and C. E. Myers, *J. Biol. Chem.*, 1985, **260**, 68206; Z. Ma, B. Zhao and Z. Yuan, *Anal. Chim. Acta.*, 1999, **389**, 213.
11 F. A. Villamena, C. M. Hadad and J. L. Zweier, *J. Am. Chem. Soc.*, 2004, **126**, 1816.
12 J. L. Zweier, J. T. Flaherty and M. L. Weisfeldt, *Proc. Natl. Acad. Sci. USA*, 1987, **84**, 1404; S. Sankarapandi and J. Zweier, *J. Biol. Chem.*, 1999, **274**, 34576.
13 F. A. Villamena, C. M. Hadad and J. L. Zweier, *J. Phys. Chem. A*, 2005, **109**, 1662.
14 F. A. Villamena, A. Rockenbauer, J. Gallucci, M. Velayutham, C. M. Hadad and J. L. Zweier, *J. Org. Chem.*, 2004, **69**, 7994.
15 Y. Kotake and E. G. Janzen, *J. Am. Chem. Soc.*, 1991, **113**, 9503–9506.
16 K. Saito and R. G. Cutler, *Oxidative Stress and Aging*, Birkhauser, Basel, Switzerland, 1995, p. 379.
17 W. Chamulitrat, C. E. Parker, K. B. Tomer and R. P. Mason, *Free Radical Res.*, 1995, **23**, 1.
18 E. Finkelstein, G. M. Rosen and E. J. Rauckman, *Mol. Pharmacol.*, 1982, **21**, 262.
19 P. Bilski, K. Reszka, M. Bilska and C. F. Chignell, *J.Am. Chem. Soc.*, 1996, **118**, 1330.
20 K. Hiramoto, Y. Ryuno and K. Kikugawa, *Mutat. Res.*, 2002, **520**, 103.
21 R. A. Floyd and K. Hensley, *Ann. N. Y. Acad. Sci.*, 2000, **899**, 222–237.
22 O. Inanami and M. Kuwabara, *Free Radical Res.*, 1995, **23**, 33–39.
23 A. R. Green, *Crit. Rev. Neurobiol.*, 2004, **16**, 91; Z. Zhao, M. Cheng, K. R. Maples, J. Y. Ma and A. M. Buchan, *Brain Res.*, 2001, **909**, 46.
24 D. A. Becker, J. J; Ley, L. Echegoyen and R. Alvarado, *J. Am. Chem. Soc.*, 2002, **124**, 4678; M. D. Ginsberg, D. A. Becker, R. Busto, A. Belayev, Y. Zhang, L. Khoutorova, J. J. Ley, W. Zhao and L. Belayev, *Ann. Neurol.*, 2003, **54**, 330.
25 K. Tsuchiya, J.-J. Jiang, Y. Masanori, T. Tamaki, H. Houchi, K. Minakuchi, K. Fukuzawa and R. P. Mason, *Free Radical Biol. Med.*, 1999, **27**, 347.
26 Y. Xia, A. J. Cardounel, A. F. Vanin and J. L. Zweier, *Free Radical Biol. Med.*, 2000, **29**, 793.
27 S. Venkataraman, S. M. Martin, F. Q. Schafer and G. R. Buettner, *Free Radical Biol. Med.*, 2000, **29**, 580–585.
28 F. A. Villamena, J. K. Merle, C. M. Hadad and J. L. Zweier, *J. Phys Chem. A*, 2005, **109**, 6083–6088.
29 F. A. Villamena, J. K. Merle, C. M. Hadad and J. L. Zweier, *J. Phys Chem. A.*, 2005, **109**, 6089–6098.
30 M. H. Holschbach, D. Sanz, R. M. Claramunt, L. Infantes, S. Motherwell, P. R. Raithby, M. L. Jimeno, D. Herrero, I. Alkorta, N. Jagerovic and J. Elguero, *J. Org. Chem.*, 2003, **68**, 8831–8837.
31 P. G. Wang, M. Xian, X. Tang, X. Wu, Z. Wen, T. Cai and A. J. Janczuk, *Chem. Rev.*, 2002, **102**, 1091–1134 reference therein.
32 P. Arranz Mascaros, M. D. Gutierrez Valero, J. N. Low and C. Glidewell, *Acta. Crystallogr., Sect. C*, 2003, **59**, 210.
33 S. Pou, Y. I. Huang, A. Bhan, V. S. Bhadti, R. S. Hosmane, S. Y. Wu, G. L. XCao and G. M. Rosen, *Anal. Biochem.*, 1993, **212**, 85; G.-M. Luo, D.-H. Qi, Y.-G. Zheng, Y. Mu, G.-I. Yan, T.-S. Yang and J.-C. Shen, *FEBS Lett.*, 2001, **492**, 29; J. M. Downey, D. J. Hearse and D. M. Yellon, *J. Mol. Cell. Cardiol.*, 1988, **20**(Suppl. 2), 55.
34 G. R. Buettner and L. W. Oberley, *Biochem. Biophys. Res. Commun.*, 1978, **83**, 69.
35 N. V. Blough and O. C. Zafiriou, *Inorg. Chem.*, 1985, **24**, 3502.
36 M. Du, W. Wu, N. Ercal and Y. Ma, *J. Chromatogr., B: Anal. Technol. Biomed. Life Sci.*, 2004, **803**, 321; J. P. Crow and J. S. Beckman, *Methods: A Companion to Methods in Enzymology*, 1995, **7**, 116; K. A. Skinner, J. P. Crow, H. B. Skinner, R. T. Chandler, J. A. Thompson and D. A. Parks, *Arch. Biochem. Biophys.*, 1997, **342**, 282.
37 J. S. Stamler, D. J. Singel and J. Loscalzo, *Science*, 1992, **258**, 1898.
38 K. Rejdak, A. Petzold, M. A. Sharpe, M. Smith, G. Keir, Z. Stelmasiak, E. J. Thompson and G. Giovannoni, *J. Neurol. Sci.*, 2003, **208**, 1; P. Kleinbongard, T. Rassaf, A. Dejam, S. Kerber and M. Kelm, *Method. Enzymol.*, 2002, **359**, 158.
39 P. Astolfi, L. Greci and M. Panagiotaki, *Free Radical Res.*, 2005, **39**, 137.
40 T. Ozawa, Y. Miura and J.-I. Ueda, *Free Radical Biol. Med.*, 1996, **20**, 837.
41 J. M. Fukuto, A. J. Hobbs and L. J. Ignarro, *Biochem. Biophys. Res. Commun.*, 1993, **196**, 707.
42 J. L. Zweier, A. Samouilov and P. Kuppusamy, *Biochim. Biophys. Acta*, 1999, **1411**, 250–262; M. N. Hughes and H. G. Nicklin, *J. Chem. Soc. A*, 1968, **2**, 450.
43 W. Braida and S. K. Ong, *Water, Air, Soil Pollut.*, 2000, **118**, 13–26.
44 V. V. Nikonorov and T. A. Belyanskaya, *J. Anal. Chem.*, 2000, **55**, 116.
45 L. A. Shinobu, S. G. Jones and M. M. Jones, *Acta. Pharmacol. Toxicol.*, 1984, **54**, 189.
46 P. Marcolongo, R. Fulceri, R. Giunti, A. Burchell and A. Benedetti, *Biochem. Biophys. Res. Commun.*, 1996, **219**, 916–922.
47 A. Kezler, B. Kalyanaraman and N. Hogg, *Free Radical Biol. Med.*, 2003, **35**, 1149–1157.